Journal of Ceramic Processing Research. Vol. 12, No. 6, pp. 615~623 (2011)

J O U R N A L O F
Ceramic Processing Research

Reinforcing of extruded ceramic Raschig rings by dispersive particles: the effects of alumina and zirconium silicate on the reliability of a ceramic body

A. Salem* and S. Shirchi
Mineral Processing Research Center, Chemical Engineering Department, Sahand University of Technology, Tabriz, Iran

Most packed beds contain heterogeneous microstructures with relatively big defects and pores, causing a large reduction in compressive strength and reliability. Recently, the need for fabricating reliable ceramic Raschig rings with high strength has increased due to their applications in processes where a high diametrical stress is applied. In manufacturing these materials, the strength and reliability are basically affected by the mixing ratio of reinforcing materials such as alumina and zirconium silicate. However, the firing process should be controlled to achieve the desired properties. Therefore, the objective of this investigation was to evaluate the firing behavior, technological properties and microstructure of a typical extruded ceramic Raschig ring. The technological properties of rings prepared with different amounts of alumina and zirconium silicate sintered at 1150, 1200 and 1250 °C were evaluated by measuring the shrinkage, water absorption, porosity and strength. The reliability of rings was studied by Weibull's statistical theory. The results showed that the addition of 10% alumina or 5% zirconium silicate into the ring composition improves the Weibull modulus considerably. Finally, the optimum particle size of alumina was determined to improve the mechanical characteristics. It was found to be less than 38 μm. The results obtained can be useful in industrial applications.

Key words: Ceramics, Sintering, Mechanical properties, Defects.

Introduction

The required technical performance of ceramic beds is normally associated with water absorption, compressive strength and reliability [1]. These properties largely depend on microstructural characteristics such as defects, porosity and second phase formation [2]. The final microstructure of these ceramic beds is essentially affected by shaping and densification processes in which physical and chemical reactions occur in the ceramic body [3]. Ceramic beds are normally composed of two types of raw materials: plastic and non-plastic materials [4]. The plastic materials are predominantly based on kaolin or illitic-kaolinitic clays which are necessary to develop the plasticity as well as to obtain satisfactory green and dry mechanical strength. The non-plastic materials are divided into two groups: fluxing agents and fillers [5]. The fluxing agents such as feldspars and nepheline syenite are used in small amounts due to decreasing thermal and chemical resistances of a packed bed during chemical processes such as distillation, absorption and chemical reactions [6]. Fillers such as quartz, alumina and zirconium silicate normally are added to ceramic body compositions to reinforce the matrix [7].

A significant improvement in physical-mechanical characteristics has been achieved by dispersing second phases of different materials. On the basis of previously studies, new classes of materials with enhanced strength and reliability have been developed. Harada *et al*. showed that the addition of alumina to a feldspathic body can raise the flexural strength [7]. Also, they indicated that the flexural strength of specimens linearly increases with the amount of alumina and the maximum strength was achieved in the presence of fine particles, around 1-2 μm. The results obtained by Chen *et al*. demonstrated that mullite can be prepared by a reaction between kaolinite and alumina that the alumina particles are inert to kaolinite below 1200 °C [8]. Also, the reaction between alumina and a glass phase to form mullite starts from 1300 °C. Regarding the kaolin-alumina reaction during the sintering process Chen *et al*. reported that the average pore size of specimens prepared by mixing 60 wt.% kaolin and 40% alumina increases from 0.6 to 1.5 μm as a function of temperature [9]. The XRD results showed that the content of mullite obtained from the kaolinite-alumina reaction shifted to larger values in the temperature range of 1300-1550 °C, reflecting the growth of crystalline phase. In the study presented by Esposite *et al*. the influence of a partially addition of stabilized zirconia powder to a porcelain stoneware composition was investigated [10]. The addition of zirconia powder into the mix leads to improved strength and reliability as a result of a more homogeneous microstructure.

It is well known that the ceramic packed beds have to be considered as materials in which the synergy of fabrication technology and physical-mechanical characteristics should reach excellent levels. This type of ceramic

*Corresponding author:
Tel : +98-412-3459145
Fax: +98-412-3444355
E-mail: salem@sut.ac.ir

products is characterized by a very compact structure with high compressive strength and reliability. Therefore, further improvement in mechanical characteristics should be achieved with reinforcing materials and the sintering process.

The purpose of this investigation is to fabricate a new ceramic pack bed in the shape of a Raschig ring that is characterized by high compressive strength and reliability which is manufactured using low amounts of reinforcing materials such as alumina and zirconium silicate without the addition of fluxing agents. The mechanical strength and reliability of the resultant Raschig rings are also studied by statistical Weibull theory with different contents of alumina and zirconium silicate.

Materials and Methods

Industrial kaolin which consists of kaolinite, pyrophilite, illite and quartz was selected as the base raw material, STD. Also alumina and zirconium silicate powder (particle size less than 38 μm) were used in the preparation of ceramic compositions. Table 1 shows the chemical analysis of the kaolin used and its X-ray pattern is shown in Fig. 1. The kaolin employed in this study was an illitic-kaolinitic clay used in the fabrication of ceramic bodies by Iranian ceramic industries. 5 and 10 wt.% of alumina, denoted as C_1 and C_2, and the same amounts of zirconium silicate, denoted as C_3 and C_4, were separately added to the kaolin to obtain the modified compositions. For the preparation of pastes, the starting and modified compositions were mixed with 30 wt.% distilled water. The pastes were left for 48 hours to produce compositions with homogenous moisture content. De-airing of paste was carried out in a laboratory pug mill and repeated two times for each composition to obtain uniform pastes. Hollow cylindrical specimens, named Raschig rings, with dimensions reported in Table 2 were fabricated using laboratory single screw extruder at a pressure of 20 MPa. These specimens were dried at 100 °C for 24 hours in an electrical oven. The extrusion behavior was evaluated by determining bulk density and total porosity. These parameters were measured using calipers accurate to 0.1 mm, determining the bulk density from specimen geometrical dimensions and weights.

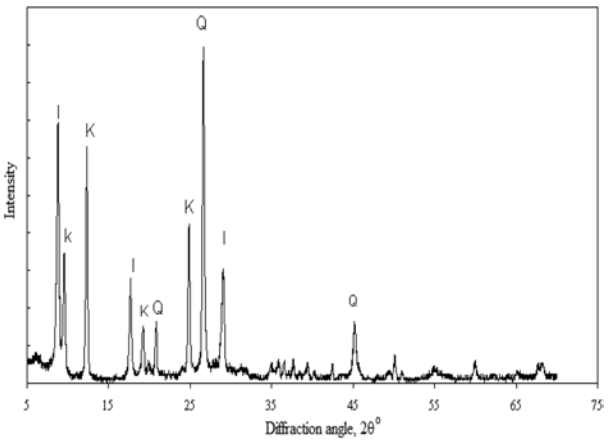

Fig. 1. The XRD pattern of the kaolin used as the base material.

True densities of clay, alumina and zirconium silicate powders were determined by a helium pycnometer. The total porosity was calculated as a follows:

$$\text{total porosity} = 1-\frac{\text{bulk density}}{\text{true density}} \quad (1)$$

The dry specimens were subsequently fired at temperatures varying from 1150 to 1250 °C in steps of 50 °C in an electrical kiln (Model EX. 1500-6L, Iran) with two hours soaking at the maximum temperature. The cooling of specimens was performed by natural convection after turning off the kiln and leaving the specimens inside. The fired technological properties were evaluated by measuring linear shrinkage, water absorption, open, total and closed porosity. These parameters were measured by standard methods [11, 12].

The diametric compressive strength tests were performed with a universal machine (Model Adamel Lhomargy DY-26, France). In order to better understand the effect of reinforcement materials on reliability of ceramic Raschig rings, Weibull statistical analysis was used to analyze each set of strength data by following equation [13] :

$$P_n = 1-exp\left[-\left(\frac{\sigma-\sigma_t}{\sigma_0}\right)^m\right] \quad (2)$$

Table 1. The chemical analysis of the kaolin used

Oxides	SiO_2	Al_2O_3	Fe_2O_3	TiO_2	CaO	MgO	K_2O	Na_2O	SO_3	L.O.I
Percentage	58.00	28.00	0.35	<0.25	<0.50	<0.15	4.50	<0.20	trace	6.00

Table 2. The geometrical dimensions and physical properties of dry rings

Composition	Reinforcement (%)	Internal diameter (cm)	External diameter (cm)	Length (cm)	Bulk density (gr/cm^3)	Total porosity (%)
STD		1.49 ± 0.00	2.46 ± 0.01	2.52 ± 0.04	1.63 ± 0.03	34.5 ± 1.2
C_1	5 Al_2O_3	1.49 ± 0.01	2.45 ± 0.01	2.54 ± 0.03	1.68 ± 0.02	33.9 ± 0.8
C_2	10 Al_2O_3	1.49 ± 0.00	2.45 ± 0.01	2.51 ± 0.04	1.72 ± 0.02	33.6 ± 0.8
C_3	5 $ZrSiO_4$	1.49 ± 0.00	2.45 ± 0.01	2.49 ± 0.04	1.72 ± 0.02	32.6 ± 0.8
C_4	10 $ZrSiO_4$	1.49 ± 0.00	2.46 ± 0.01	2.49 ± 0.03	1.71 ± 0.02	34.5 ± 0.8

where P_n is the probability of failure, σ is the fracture stress, σ_t is the threshold stress which is zero for brittle materials such as ceramics, σ_0 is a scaling parameter and selected as the characteristic stress in which the probability of failure is 63.2%, m is the Weibull modulus which describes the narrowness of failure. The probability of failure can be found from different probability estimators. In this investigation the following equation was selected to calculate the value of P_n [14] :

$$P_n = \frac{1}{N+1} \tag{3}$$

where N is the number of specimens used in strength tests and n is the ranking number, with $n = 1$ for the weakest specimen and $n = N$ for the strongest sample. The Weibull modulus, m, and scaling parameter, σ_0, can be evaluated by a logarithmic form of Equation 2 as a follows:

$$\ln[-\ln(1-P_n)] = m\ln\sigma - m\ln\sigma_0 \tag{4}$$

The mineralogical analyses of specimens fired at different temperatures were performed by X-ray diffraction (Model D5000 Siemens, Germany). Scanning electron microscopy, SEM, observation of gold coated specimens of fired ceramic fracture surfaces was carried out to evaluate the defects and morphology of pores (Model EOL-4401, England). The above procedures were repeated for specimens prepared with alumina powders with particle size distributions of > 75 μm (+200 mesh) and 38-75 μm (–200 to 400 mesh) to evaluated the effect of the particle size of alumina on reliability of ceramic Raschig rings.

Results and Discussion

Table 2 presents the dry bulk densities and total porosity of STD and modified compositions. These data indicate that bulk density of all compositions prepared with alumina and zirconium silicate are more than that for the STD composition and reaches a maximum value of 1.72 g/cm^3. It is obvious that the value of bulk density remains approximately constant for all compositions prepared with the $ZrSiO_4$ powder. When the amounts of Al_2O_3 and $ZrSiO_4$ rise to 10 and 5 wt.% respectively, although this difference is not considerable, the maximum voids are sufficient to be occupied by Al_2O_3 and $ZrSiO_4$ particles. A large amount of $ZrSiO_4$ causes an expanded particle rearrangement. For this reason the specimens formed with 10% $ZrSiO_4$ exhibited a little higher porosity.

Fig. 2 presents the behavior of linear shrinkage as a function of the firing temperature for bodies containing different amounts of Al_2O_3 and $ZrSiO_4$. It can be seen that a similar behavior with a comparatively linear shrinkage variation at 1200 ºC in the presence 10 wt.% of Al_2O_3. Also, the shrinkage of ceramic bodies is affected negligibly by the $ZrSiO_4$ content.

Fig. 3 presents the water absorption as a function of the firing temperature for all the investigated bodies. It

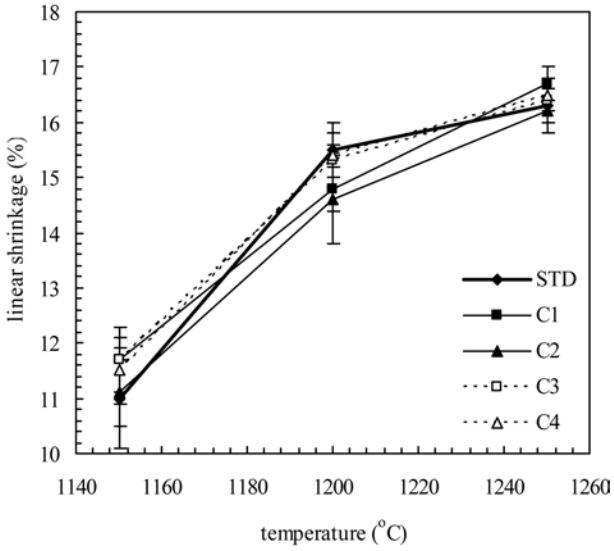

Fig. 2. The variation of linear shrinkage as a function of the sintering temperature for the reference and modified compositions.

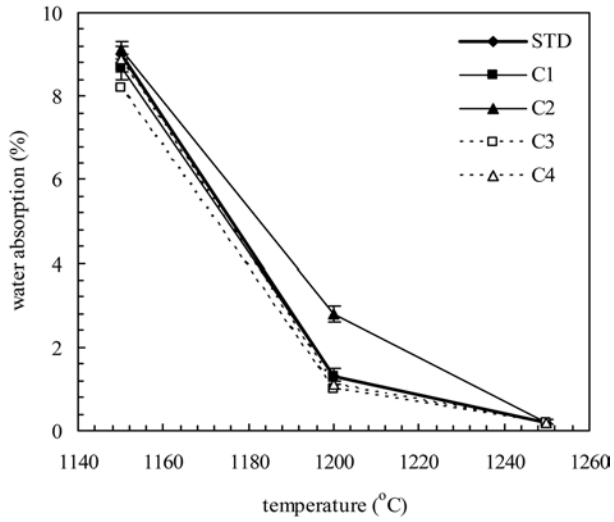

Fig. 3. The variation of linear water absorption as a function of the sintering temperature for the reference and modified compositions.

is observed that all bodies show a decrease in water absorption with an increase in the temperature. This is a consequence of a reduction in the open porosity associated with liquid phase formation during the sintering process. As is shown, there are some differences between the three plots, although they are roughly similar in behavior. The water absorption of the body containing 10 wt.% Al_2O_3 is also different at 1200 ºC. These results are indicative of their different sinterability. As is generally known, Al_2O_3 powder is more sinterable than $ZrSiO_4$ powder. The sinterability of the bodies mainly depends on the Al_2O_3/clay and $ZrSiO_4$/clay ratios, and more desirable sinterability can be obtained if the firing temperature is increased up to 1250 ºC. The water absorption approximately remains the same for STD and compositions containing 5 and 10 wt.% $ZrSiO_4$ at all of the sintering temperatures. In

particular, the bodies containing $ZrSiO_4$ give the same behavior which can be attributed to their more refractory behavior at temperatures lower than 1250 °C. By contrast with bodies containing $ZrSiO_4$, the specimens prepared with the addition of 10 wt.% Al_2O_3 present a considerable increment in water absorption at 1200 °C.

The total and closed porosity of ceramic Raschig rings prepared with the addition of Al_2O_3 and $ZrSiO_4$ are reported in Table 3. With an increase in the sintering temperature, the total porosity of the STD composition decreases, reaching to near the value of the closed porosity when the open porosity is near to zero at 1250 °C. Similar trends are also observed, for compositions containing Al_2O_3 and $ZrSiO_4$. The total porosity decreases to reach a minimum value at 1250 °C and remains approximately near the closed porosity. The values of total and closed porosity of bodies containing 10 wt.% Al_2O_3 and 5% $ZrSiO_4$ are approximately equal at 1250 °C, in agreement with a more effective packed structure following the same trends for dry porosity. Therefore, the differences between the porosity should be directly related to the green shaping condition.

The presence of Al_2O_3 substantially changes the values of total and closed porosity when the sintering process is carried out at 1200 °C, particularly in the body containing 10 wt.% Al_2O_3 due to its more refractory behavior. On the other hand, Al_2O_3 seems to decrease the larger amount of closed porosity at 1250 °C. This tendency is also particularly conspicuous in bodies containing 5 and 10 wt.% $ZrSiO_4$ comparing to the STD composition at this temperature. Regardless, the effect of the green forming process on the compaction of a sintered body, the large value of total porosity in the STD body sintered at 1250 °C may be due to overfiring of the body at this temperature.

The values of compressive diametric strength as a function of the firing temperature for all studied compositions are summarized in Table 4. It should be remembered that the mechanical strength strongly depends on the microstructure of a ceramic body, especially defects such as pores and cracks. Furthermore, the data of Table 4 shows that all the bodies give an increase in strength with the firing temperature. The maximum strength is observed in bodies containing 10 0wt.% Al_2O_3 and 5 wt.% $ZrSiO_4$ respectively, at 1250 °C, due to lower porosity compared to the STD composition and particle dispersive reinforcement. This behavior at 1250 °C can be attributed to a low porosity.

Table 3. The total and closed porosity of reference and modified rings

Composition	Reinforcement (%)	Total porosity (%)			Closed porosity (%)		
		1150 °C	1200 °C	1250 °C	1150 °C	1200 °C	1250 °C
STD		19.9 ± 0.4	6.4 ± 0.3	5.5 ± 0.3	1.9 ± 0.4	3.4 ± 0.3	5.0 ± 0.3
C_1	5 Al_2O_3	19.1 ± 0.4	7.4 ± 0.2	4.7 ± 0.2	1.0 ± 0.4	4.5 ± 0.2	4.2 ± 0.2
C_2	10 Al_2O_3	18.9 ± 0.3	8.9 ± 0.2	3.8 ± 0.3	0.7 ± 0.3	2.5 ± 0.2	3.3 ± 0.3
C_3	5 $ZrSiO_4$	18.2 ± 0.3	6.3 ± 0.2	3.9 ± 0.2	0.7 ± 0.3	3.8 ± 0.2	3.4 ± 0.2
C_4	10 $ZrSiO_4$	19.5 ± 0.3	6.6 ± 0.3	4.2 ± 0.2	0.8 ± 0.3	4.2 ± 0.3	3.6 ± 0.2

Table 4. The average compressive strength and parameters of the Weibull distribution as a function of temperature for the reference and modified rings

Composition	Reinforcement (%)	Temperature (°C)	Average strength (MPa)	Weibull modulus	Scaling factor (MPa)	R[a]
STD		1150	9.9 ± 1.4	8.0	10.5	0.93
		1200	19.0 ± 3.7	5.6	20.6	0.96
		1250	30.8 ± 6.7	5.1	33.5	0.98
C_1	5 Al_2O_3	1150	12.9 ± 1.6	8.9	13.6	0.98
		1200	20.7 ± 3.3	6.6	22.1	0.98
		1250	30.8 ± 7.7	4.5	33.8	0.92
C_2	10 Al_2O_3	1150	12.8 ± 1.7	8.3	13.5	0.98
		1200	24.9 ± 4.6	5.7	26.9	0.93
		1250	]43.4 ± 7.2	6.1	46.6	0.97
C_3	5 $ZrSiO_4$	1150	11.4 ± 1.2	10.3	11.9	0.97
		1200	27.5 ± 4.6	6.2	29.6	0.96
		1250	39.1 ± 5.2	6.4	34.4	0.94
C_4	10 $ZrSiO_4$	1150	12.7 ± 1.4	9.7	13.3	0.93
		1200	22.2 ± 3.1	7.4	23.6	0.98
		1250	31.2 ± 4.4	7.6	33.1	0.97

[a]Linear correlation coefficient

The value of porosity in the presence 10% Al_2O_3 at 1200 ºC is more than that for the body prepared with 5% $ZrSiO_4$ therefore, the greater strength of the body containing 5% $ZrSiO_4$ could be attributed to the low value of porosity. Also, Al_2O_3 and $ZrSiO_4$ are often used as reinforcements with regard to particle dispersed reinforcement. The dispersive particles limit the possible size of the flaws. On the other hand, the dispersed particles increase the fracture energy by an interaction between the dispersed particles and propagating crack fronts. At higher sintering temperatures mullite and residual quartz crystals dispersed in a vitreous matrix are expected to be formed. This aspect will be later discussed by in terms X-ray patterns.

The Weibull statistical distributions for the STD and compositions modified by Al_2O_3 and $ZrSiO_4$, shown in Fig. 4, were used to evaluate graphically the Weibull modulus and scaling stress. The values of Weibull parameters are summarized in Table 4. Five series of rings, sintered at three temperatures, show suitable fits with linear correlation coefficients of 0.93 to 0.98 therefore, a good agreement was obtained between the experimental data and the calculated values. The Weibull modulus of the STD composition shows a considerable decrease in reliability of ceramic rings with an increase in the sintering temperature, about 35%. Another interesting point concerns the compressive strength data distribution in the presence of $ZrSiO_4$. The increase in Weibull modulus at 1250 ºC, shows a decrease in the scattering of data for the materials prepared with $ZrSiO_4$. This result is due to a more homogeneous microstructure and a very good dispersion of the $ZrSiO_4$ particles in the matrix. An increase in the $ZrSiO_4$ content in the composition of a ring negatively affected the mechanical strength and the Weibull modulus did not increase sufficiently. The significant dispersion of $ZrSiO_4$ particles in the matrix of rings can be considered as a reason for the improved value of the Weibull modulus. According to Table 4 data, only the addition of 10 wt.% Al_2O_3 can improve the reliability of rings. Approximately, a 20% increment in Weibull modulus is due to a suitable dispersion of Al_2O_3 particles in the ceramic matrix.

Microstructural analyses were carried out only on

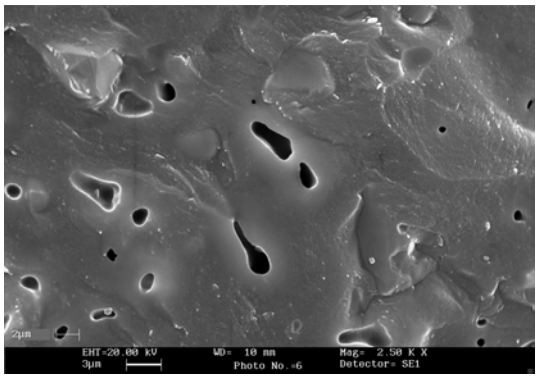

Fig. 5. SEM micrograph of a STD ring sintered at 1250 ºC.

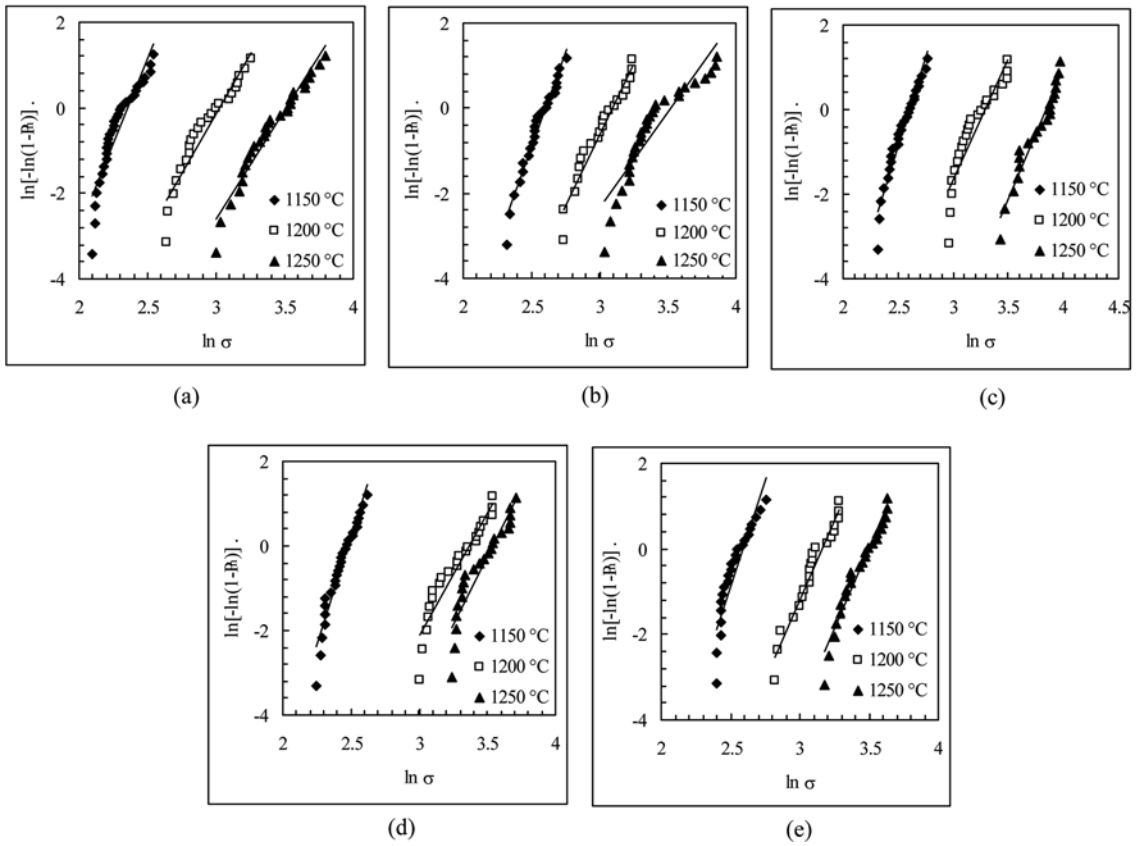

Fig. 4. Weibull distribution for the reference and modified compositions at different temperatures (a) STD, (b) C_1, (c) C_2, (d) C_3, (e) C_4.

fracture surface of bodies sintered at 1250 °C, which is a typical temperature employed to reach water absorption of about 0.2%. Fig. 5 shows the fracture surface of the STD body sintered at 1250 °C. The main feature in this microstructure is the presence of large pores that were distributed nonhomogeneously in rings structure, due to over firing of body that is frequently occurring phenomenon in ceramic bodies. Fig. 5 apparently displays a great pore that is in agreement with corresponding results on total porosity measurement.

Fig. 6 shows a compact microstructure with small defects in the presence of 10% Al_2O_3, confirming the reliability of the body. However, the use of 5% Al_2O_3 in the composition of a ceramic Raschig ring is not able to decrease the defect size during the extrusion process. Fig. 7 shows the defects of bodies containing 5 and 10% $ZrSiO_4$ fired at 1250 °C. This figure demonstrates the presence of a small defect in a body prepared with 5 wt.% $ZrSiO_4$ due to a suitable shaping process and the development of a glassy phase during the firing schedule. It is also observed that the fracture surface of the body containing 10% $ZrSiO_4$ is typically nonhomogeneous and a large defect was found compared to the body containing 5% $ZrSiO_4$ and sintered at the same temperature.

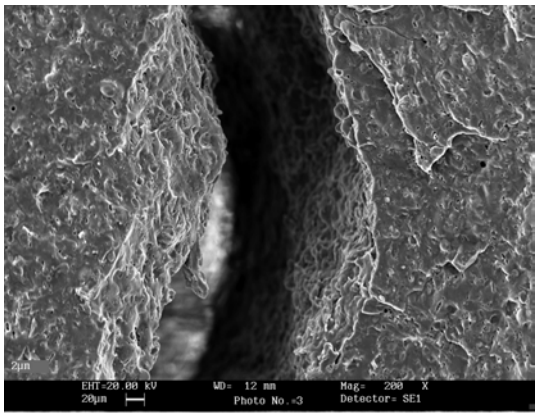

(a)

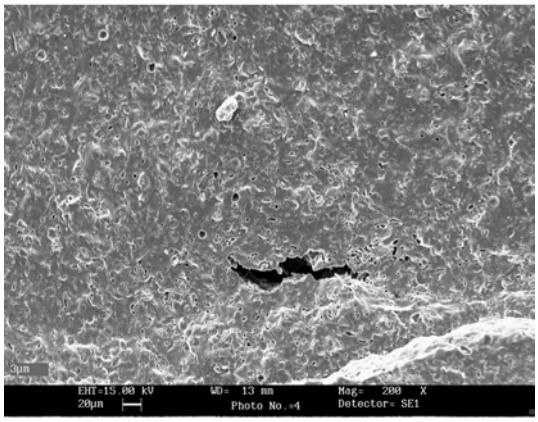

(b)

Fig. 6. The defects in sintered rings prepared with different amounts of alumina, (a) C_1 and (b) C_2.

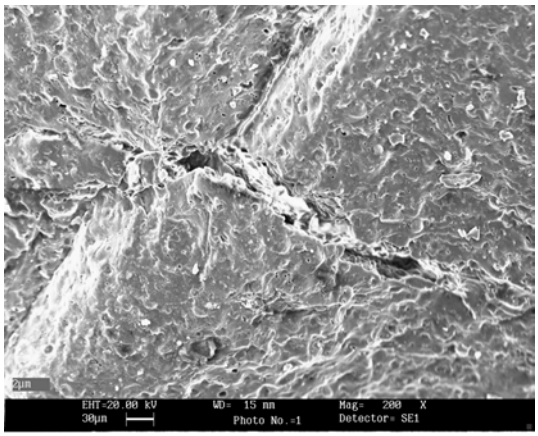

(a)

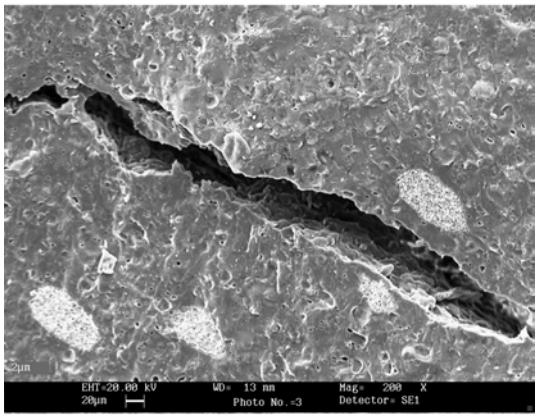

(b)

Fig. 7. The defects in sintered rings prepared by different amounts of zirconium silicate, (a) C_3 and (b) C_4.

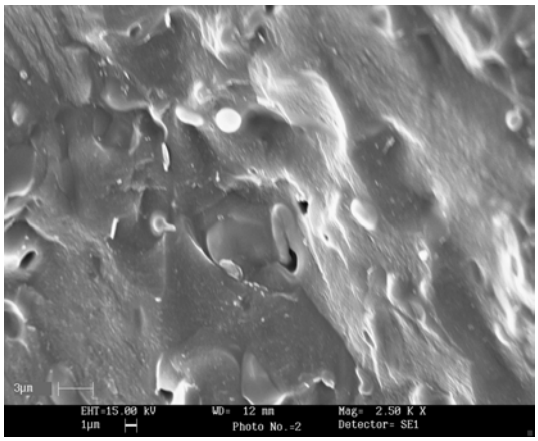

Fig. 8. SEM micrograph of a ring prepared with 10 wt.% alumina and sintered at 1250 °C.

Fig. 8 demonstrates a compacted microstructure in the presence of 10 wt.% Al_2O_3, indicating a uniform distribution of pores. This characteristic associated with strong densification due to a suitable development of a liquid phase causes an increase in the reliability of rings. Fig. 9 shows the microstructure of body containing 5 wt.% $ZrSiO_4$ sintered at 1250 °C. The presence of small pores

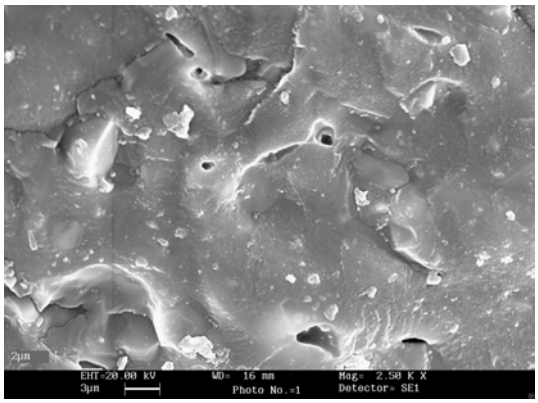

Fig. 9. SEM micrograph of a ring prepared with 10 wt.% zirconium silicate and sintered at 1250 ºC.

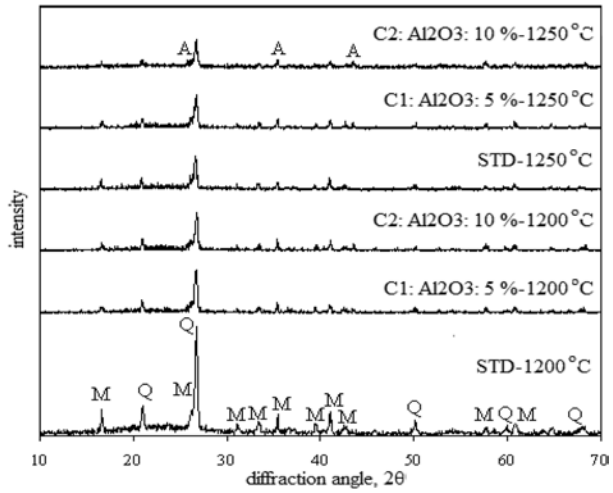

Fig. 10. XRD patterns of the reference and compositions modified by alumina sintered at 1200 and 1250 ºC. A : alumina, M : mullite and Q : quartz.

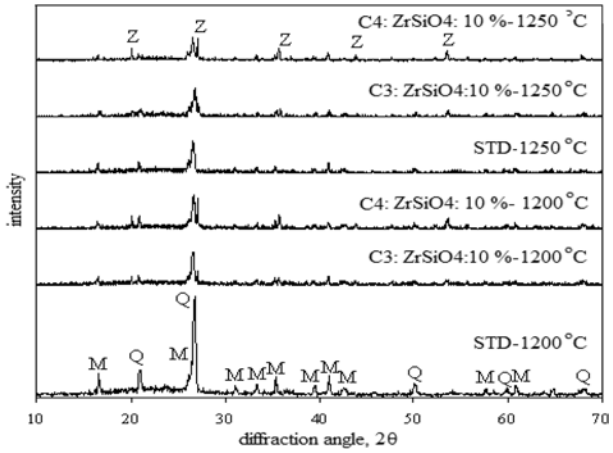

Fig. 11. XRD patterns of the reference and compositions modified by zirconium silicate sintered at 1200 and 1250 ºC. M : mullite, Q : quartz and Z : zirconium silicate.

and a uniform texture compared to the STD ring may be seen. Therefore, the Weibull modulus shows a general increase in the presence of 5 wt.% $ZrSiO_4$.

Fig. 10 shows the XRD patterns of the bodies studied containing different amounts of Al_2O_3, fired at 1200 and 1250 ºC. In general, all the bodies present similar crystalline phases. The identified common phases, found in the STD composition, were quartz and mullite. Also Al_2O_3 peaks in the XRD patterns are seen as a residual phase. From the raw materials, mullite comes from the metakaolinite decomposition around 950 ºC. This Figure also indicates the formation behavior of mullite and dissolution of quartz. The amount of mullite in the sintered rings increased slightly when the sintering temperature was raised from 1200 to 1250 ºC due to the nearly complete transformation of kaolinite. This reveals that the amount of Al_2O_3 content is not reduced and it chemically remains inert until 1250 ºC.

Fig. 11 shows the XRD patterns of ceramic bodies containing 5 and 10 wt.% $ZrSiO_4$ at different sintering temperatures. It can be observed that the crystalline phases are quartz, mullite and zirconium silicate. Quartz and zirconium silicate are residual phases i.e. components of the initial composition that did not suffer chemical transformations during the firing stages. By contrast, mullite was formed during the sintering process.

Table 5 reports the geometrical specifications of dry rings prepared with different particle sizes of Al_2O_3. From this data, it can be observed that the body containing coarse particles gives the highest bulk density of 1.75 g/cm^3. The use of coarse particles of alumina in the preparation of rings causes a small decrease in the total porosity. Thus increasing the alumina particle size produces a parallel drop in the available voids, which increases the dry density up to 1.75 g/cm^3 while the other specimens prepared with fine particles presents a low density. The variation in total porosity of dry specimens is also reported in Table 5 as a function of the particle size of Al_2O_3. It is obvious that the lowest value of the total porosity has been observed in the body prepared with coarse particles. This difference is about 1% but it should be expected that the mechanical strength is influenced by the forming process followed by a change in the particle size of reinforcing material.

Among the three alumina particle sizes, the body prepared using coarse particles partially shows greater compaction during extrusion compared to STD specimens. Therefore, it can be concluded that the specimens prepared with

Table 5. The geometrical dimensions and physical properties of dry rings prepared by different particle sizes of alumina

Particle size distribution (µm)	Internal diameter (cm)	External diameter (cm)	Length (cm)	Bulk density (gr/cm^3)	Total porosity (%)
> 75	1.49 ± 0.00	2.45 ± 0.00	2.46 ± 0.03	1.75 ± 0.01	32.4 ± 0.4
38-75	1.49 ± 0.00	2.45 ± 0.00	2.47 ± 0.03	1.75 ± 0.01	33.6 ± 0.4
< 38	1.49 ± 0.00	2.45 ± 0.01	2.51 ± 0.04	1.72 ± 0.02	33.6 ± 0.8

coarse particles of Al_2O_3 give better compaction during the extrusion.

Table 6 shows the effect of the particle size distribution of Al_2O_3 on the technical properties of ceramic Raschig rings. The shrinkage was influenced by the particle size of Al_2O_3 and reaches a maximum value when fine particles, less than 38 μm, were used. Also, the water absorption decreased as the particle size of Al_2O_3 was reduced. The tendency of total and closed porosity with particle size was similar to the variation of water absorption and indicated a maximum value when coarse particles of Al_2O_3, > 75 μm, were added to the composition. The reason for this tendency seems to be the result of different microstructures.

The SEM micrographs of the specimens prepared with coarse particles of alumina and sintered at 1250 °C are shown in Fig. 12. The observation of fracture surfaces of specimens showed microstructural defects due to the extrusion of pastes. The sizes of defects are different and change with the particle size of Al_2O_3 and reach maximum dimension when coarse particles of Al_2O_3 were used in the composition compared to Fig. 6(b). The morphology of isolated pores in the body mentioned is indicated in Fig. 13. A few closed pores were observed in the body containing fine particles of Al_2O_3, Fig. 8, which positively affects the compressive strength, Table 7. Because of the large number of pores in the body containing coarse particles it should be expected that the strength is reduced while the use of fine particles is more likely to give a compact body after densification. Regardless of the positive effect of coarse particles of Al_2O_3 on the compaction of dry specimens, the body prepared with fine particles gives the maximum strength. The maximum dry bulk density was obtained when coarse particles of Al_2O_3 were used in preparation of rings. This body contains different pores with a uniform distribution on the fracture surface compared to Fig. 8 in which fine particles were added to the body composition. The sharp and broad pores are found in this case and they were surrounded by a glassy phase. Thus the strength of rings decreases as the particle size of Al_2O_3 was shifted to a coarse size.

Fig. 14 represents Weibull distribution for specimens prepared with different particle sizes of Al_2O_3. The parameters of the Weibull equation are reported in Table 7. It is observed that an increase in the Al_2O_3 particle size causes a marginal increase in the Weibull modulus which improves the reliability of rings. Regardless of the negative effect of coarse particles of Al_2O_3 on the strength, the

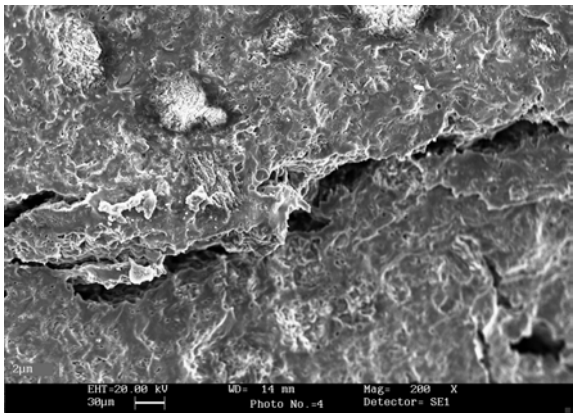

Fig. 12. The defect in ring prepared with the coarse particles of alumina, +200 mesh.

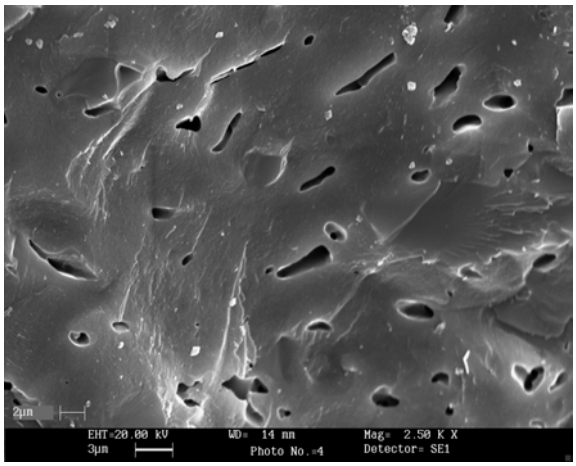

Fig. 13. The morphology of pores in ring prepared with coarse particles of alumina, +200 mesh.

Table 6. The technical characteristics of compositions prepared by addition of different particle sizes of alumina and sintered at 1250 °C

Particle size distribution (μm)	Shrinkage (%)	Water absorption (%)	Total porosity (%)	Closed porosity (%)
> 75	13.4 ± 0.2	0.61 ± 0.10	11.0 ± 0.3	9.6 ± 0.3
38-75	13.9 ± 0.3	0.70 ± 0.10	11.4 ± 0.3	9.8 ± 0.3
< 38	16.2 ± 0.4	0.20 ± 0.05	3.8 ± 0.3	3.3 ± 0.3

Table 7. The average compressive strength and parameters of Weibull distribution as function of temperature for rings prepared by different particle sizes of alumina

Particle size distribution (μm)	Average strength (MPa)	Weibull modulus	Scaling factor (MPa)	R
> 75	21.1 ± 1.8	12.4	22.0	0.96
38-75	24.4 ± 4.2	6.1	26.2	0.96
< 38	43.4 ± 7.2	6.1	46.6	0.97

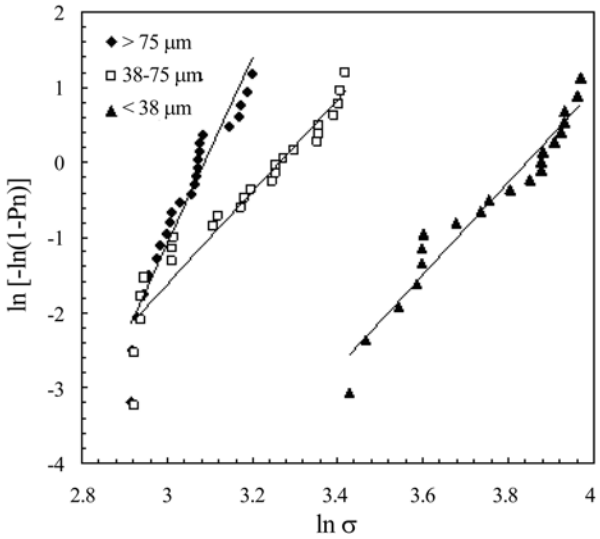

Fig. 14. Weibull distribution for rings prepared with different particle sizes of alumina and sintered at 1250 °C.

improvement in the Weibull modulus is due to the uniform distribution of pores in the cross section of Raschig rings.

Conclusions

The effects of alumina and zirconium silicate on the firing behavior, technical properties and microstructure of ceramic packed beds shaped by extrusion were investigated by fabricating ceramic Raschig rings. The following results were obtained to improve the reliability and the quality of the final products.

1. Among the various compositions used in this investigation, the rings containing 5 wt.% zirconium silicate or 10 wt.% alumina indicated the highest compressive strength which can be attributed to good interactions between a glassy phase and the reinforcing agents. Also, a decrease in defect size was the main reason for an increase of the strength. The large defects existed even at a high sintering temperature in the body prepared with 10% zirconium silicate which caused a significantly reduction in compressive strength. Although the strength of ceramic Raschig rings is improved by rising the sintering temperature, the reliability of them evaluated by Weibull statistical analysis, decreases considerably. Also, the addition of 10 wt.% alumina or 5 wt.% zirconium silicate in the composition of Raschig ring results a similar mechanical characteristics. The rings prepared with alumina are advantageous in price because the cost of alumina is cheap compared to zirconium silicate.

2. When the particle size of alumina increases to more than 75 μm, the strength reveals an opposite trend compared to the Weibull modulus. The comparative strength decreases 22 MPa approximately while the Weibull modulus is increased twice.

Acknowledgment

The author sincerely thanks Iranian Petrochemical Company and Petrochemical Research and Technology Company for financial supporting of this research.

References

1. M. Salehi and A. Salem, Korean J. Chem. Eng. 26[2] (2009) 500-505.
2. M. Salehi and A. Salem, J. Ceram. Process. Res. 9[2] (2008) 167-171.
3. M. Salehi and A. Salem, J. Mater. Process. Technol. 200 (2008) 232-237.
4. J.S. Reed, in "Introduction to Principles of Ceramic Processing" (John Wiley and Sons, 2nd ed., New York, 1995) p. 350.
5. W.M. Carty and U. Senapti, J. Am, Ceramic Soc. 81[1] (1998) 3-20.
6. N. Rostami, A. Salem and A. Paknjhad, Inter. J. Appl. Ceram. Technol. (2009) In Press.
7. R. Harada, N. Sugiyama and H. Ishida, Ceram. Eng. Sci. Proc. 17[1] (1996) 88-98.
8. C.Y. Chen, G.S. Lan and W.H. Tuan, J. Eur. Ceram. Soc. 20 (2000) 2519-2525.
9. Y.F. Chen, W.J. Shin, M.C. Wang and M.H. Hon, J. Ceram. Soc. Japan. 112 (2004) 1265-1271.
10. L. Esposito, E. Rastelli, A. Tucci and A. Albertazzi, Sil. Ind. 65[1-2] (2000) 3-6.
11. ASTM C373, in "Standard Test Method for Water Absorption, Bulk Density, Apparent Porosity and Apparent Specific Gravity of Fired Whiteware Products" (Annual Book of ASTM Standards, 2006).
12. PrEN 623-2, in "Methods of Testing Advanced Technical Ceramics General and Textural Properties, Part 2 : Determination of Density and Porosity" (Annual Book of European Standards, 1991).
13. J.M. Villora, P. Callejas and M.F. Barba, J. Eur. Ceram. Soc. 24 (2004) 589-594.
14. M. Salehi and A. Salem, in Proceedings of the Material Processing for Properties and Performance Conference, December 2006, edited by K.A. Khor, R.V. Ramanujan, C.P. Ooi and J.H. Zhao, W. Zhou and L.G. Yu (Institute of Materials, East Asia, 2006) p. 182.